J Fluoresc (2015) 25:361–367
DOI 10.1007/s10895-015-1518-0

ORIGINAL PAPER

A Magnetic Nanoparticle-Based Time-Resolved Fluoroimmunoassay for Determination of the Cytokeratin 19 Fragment in Human Serum

Guanfeng Lin · Tiancai Liu · Jingyuan Hou · Zhiqi Ren · Jianwei Zhou · Qianni Liang · Zhenhua Chen · Wenqi Dong · Yingsong Wu

Received: 11 September 2014 / Accepted: 20 January 2015 / Published online: 10 February 2015

Abstract A sensitive, rapid and novel measurement method for cytokeratin 19 fragment (CYFRA 21–1) in human serum by magnetic particle-based time-resolved fluoroimmunoassay (TRFIA) is described. Built on a sandwich-type immunoassay format, analytes in samples were captured by one monoclonal antibody coating onto the surface of magnetic beads and "sandwiched" by another monoclonal antibody labeled with europium chelates. The coefficient variations of the method were lower than 7 %, and the recoveries were in the range of 90–110 % for serum samples. The lower limit of quantitation of the present method for CYFRA 21–1 was 0.78 ng/ml. The correlation coefficient of CYFRA 21–1 values obtained by our novel TRFIA and CLIA was 0.980. The present novel TRFIA demonstrated high sensitivity, wider effective detection range and excellent reproducibility for determination of CYFRA 21–1 can be useful for early screening and prognosis evaluation of patients with non-small cell lung cancer.

Keywords Magnetic nanoparticles · Time-resolved fluoroimmunoassay · Cytokeratin 19 fragment

Abbreviations

NSCLC	Non-small cell lung cancer
CYFRA 21–1	Cytokeratin 19 fragment
TRFIA	Time-resolved fluoroimmunoassay
BSA	Ovine serum albumin
MES	4-morpholineethanesulfonic acid
NHS	N-hydroxysulfosuccinimide
EDC	1-ethyl-3-(3-dimethylaminopropyl) carbodiimide hydrochloride
Eu	Europium
CLIA	Chemiluminescence immunoassay
McAb	Monoclonal antibody
LLOQ	Lower limit of quantitation
RE	Relative error
CV	Coefficient of variation
SD	Standard deviation

G. Lin · T. Liu · J. Hou · Z. Ren · J. Zhou · Q. Liang · Z. Chen · Y. Wu (✉)
Institute of Antibody Engineering, School of Biotechnology, Southern Medical University, Guangzhou, China
e-mail: wg@smu.edu.cn

W. Dong (✉)
Department of Biopharmaceutical, School of Biotechnology, Southern Medical University, Guangzhou, China
e-mail: dongwq63@263.net

Introduction

Lung cancer is the most prevalent and generally has a very poor prognosis worldwide, and non-small cell lung cancer (NSCLC) accounted for about 85 % of lung cancer cases [1]. Approximately 20 % of patients present with stage I disease [2]. The survival of patients with stage I NSCLC is reported to be 60–85 % [2, 3]. By improving prognosis, early diagnosis is paramount to improve the survival of lung cancer patients at present [4, 5]. Additionally, these results indicate that the other 15–30 % may have tumor cells that have spread to lymph nodes or other tissues, and currently available clinical practices have failed to detect these micrometastasis, although pathologically stage I NSCLC is considered to be able to be performed complete resection [6]. Thus, it appears that a more efficient detection method such as using serum tumor markers to help the early screening of NSCLC, and select the

optimal treatment modality for individual lung cancer patients, including the use of adjuvant chemotherapy [7].

Serum tumor markers are non-invasive diagnostic tools for identifying malignant tumors, and are commonly used for the early screening of cancer and as an indicator of treatment efficacy. Cytokeratin 19 fragment (CYFRA 21–1) is a cytokeratin expressed in simple epithelium, including the bronchial epithelium, and in malignant tumor derived from these cells. CYFRA 21–1 is the most sensitive tumor marker for NSCLC, particularly squamous cell tumors [8]. A recent analysis of pooled data from nine centers demonstrated CYFRA 21–1 to be an independent prognostic factor in both early and late stages of NSCLC [9], confirming earlier multivariate studies demonstrating its prognostic relevance [10–12]. Other reports have suggested CYFRA 21–1 may also have prognostic value in SCLC [13, 14]. A number of assay methods for CYFRA 21–1 have been reported, including radioimmunoassay [9, 15], enzymelinked immunosorbent assay [16, 17], and electrochemiluminescence immunoassay [18, 19]. These methods have a number of disadvantages including radiation hazards, short half-life of iodinated labels for radioimmunoassay, low sensitivity and instability for enzymelinked immunosorbent assay, and expensive and difficult for electrochemiluminescence immunoassay to set up an open system. Time-resolved fluoroimmunoassay (TRFIA) using lanthanide complexes chelates as the labels was used as an 'ideal' immunoassay method when it was first reported by Lovgren et al. [20]. Time-resolved fluorometry of lanthanide chelates has turned out to be one of the most successful non-isotopic detection techniques, and has been noticed as a highly sensitive method and employed in numerous applications in the biomedical sciences [21–28]. We first reported the application of magnetic nanoparticles in TRFIA [29]. The combination of TRFIA and magnetic nanoparticles improves sensitivity and significantly reduces the analysis time via a homogenous format, and provides an interesting alternative tool for the determination of serum tumor markers in clinical laboratories [29–32].

We innovatively developed a novel magnetic nanoparticle-based TRFIA, which was designed specifically as a sensitive, precise and rapid measurement method for the early screening and prognosis evaluation of patients with NSCLC. Thus, the purpose of the present study was to develop a novel magnetic nanoparticle-based TRFIA and test its application for the determination of CYFRA 21–1 in human serum. This study involved measurement of parameters, such as repeatability, recovery, linearity and feasibility.

Experimental

Reagents and Instrumentation

Bovine serum albumin (BSA), 4-morpholineethanesulfonic acid (MES), N-hydroxysulfosuccinimide (NHS), 1-ethyl-3-(3-dimethylaminopropyl) carbodiimide hydrochloride (EDC), proclin-300 and Tween-20 were purchased from Sigma-Aldrich (St. Louis, MO, USA). Sephadex G-50 was purchased from Amersham Pharmacia Biotech (Piscataway, NJ, USA). All other chemicals used were of analytical reagent grade and ultra-pure water obtained using a Milli-Q water purification system (Millipore, Bedford, MA, USA) was used throughout the experiments. Anti-CYFRA 21–1 monoclonal antibodies (McAbs) (clone 1602 and 1605) were likewise obtained from Medix (Grankulla, Finland). CYFRA 21–1 antigen was purchased from BioDesign (Memphis, TN). Magnetic nanoparticles (1101GA-03) were obtained from JSR Life Sciences (Tokyo, Japan). A Victor^3 1420 Multilabel Counter for spectral analysis of fluorescent chelates, europium (Eu) labeled kits were purchased from PerkinElmer Life and Analytical Sciences (Waltham, MA, USA).

Buffer solutions used in the study were coating buffer (0.1 mol/LMES, pH 5.0); labeling buffer (50 mmol/L Na_2CO_3-$NaHCO_3$, containing 0.9 % NaCl, pH 9.0); assay buffer (25 mmol/LTris–HCl, containing 0.02 % BSA, 0.09 % NaCl, 0.05 % Tween-20 and 0.05 % proclin-300, pH 7.8); elution buffer (50 mmol/L Tris–HCl, containing 0.9 % NaCl and 0.05 % proclin-300, pH 7.8); washing buffer (50 mmol/L Tris–HCl, containing 0.9 % NaCl, 0.2 % Tween-20 and 0.05 % proclin-300, pH 7.8), standard buffer (50 mmol/L Tris–HCl, 0.2 % BSA and 0.1 % NaN_3, pH 7.8), and blocking buffer (5 % BSA, pH 7.0).

Coating Conjugate Preparation

Covalent conjugation between magnetic nanoparticles and anti-CYFRA 21–1 McAb (clone 1602) was carried out as described in our previous work. Briefly, 500 μL of magnetic nanoparticles (20 mg/mL, 2.0×10^9 magnetic nanoparticles/mL in H_2O) was suspended in 500 μL coating buffer. Then, 25 μL of EDC (10 mg/mL) and 40 μL of NHS (10 mg/mL) freshly prepared were added into the above magnetic nanoparticles suspension and the resultant mixtures were incubated at room temperature under gentle stirring to activate the carboxylic acid groups on the surface of the magnetic nanoparticles. After incubation for 30 min, the activated magnetic nanoparticles were magnetically isolated, followed by rinsing with coating buffer three times. Subsequently, 100 μg anti-CYFRA 21–1 McAb (clone 1602) was added to the activated magnetic nanoparticles in 1 mL coating buffer. The reaction proceeded at room temperature for 18 h under gentle stirring and the mixtures were subsequently rinsed four times with assay

buffer to remove unbound antibody using magnetic separation. The resultant magnetic nanoparticles were resuspended in 1 mL blocking buffer at room temperature for another 3 h to eliminate nonspecific binding effects and block the remaining active groups. After a final rinsing with assay buffer, the magnetic nanoparticles–antibody conjugates were resuspended in assay buffer and stored at 4 °C until use.

Antibody Labeling

Anti-CYFRA 21–1 McAb (clone 1605) was labeled with Eu^{3+}-chelates using the labeling buffer. Anti-CYFRA 21–1 McAb (clone 1605) was gently mixed in 200 μL of labeling buffer with 500 μg of Eu^{3+}-chelates in 100 μL of the same buffer. After an 18-h incubation with continuous gently shaking at room temperature, free Eu^{3+}-chelates and aggregated McAb were separated from Eu^{3+}-McAb conjugates using a 1 cm×40 cm column packed with sepharose CL-6B (lower 20 cm), eluted with a descending elution buffer, and collected with 1.0 mL per fraction. The concentration of Eu^{3+}-conjugates in collected fraction was measured with fluorescence, and diluted with an enhancement solution (1:1000). The fluorescence in microtitration wells (200 μL per well) was detected by comparing the signal of samples to that of stock standards diluted at 1:100 in an enhancement solution. The fractions from the first peak with the highest Eu^{3+} count were pooled and characterized. The labeled McAb was rapidly lyophilized under high vacuum after dilution with the elution buffer containing 0.2 % BSA as a stabilizer, and stored at −20 °C. No loss of immunoreactivity was observed during a 6-months storage period.

Preparation of CYFRA 21–1 Standards

The concentrations of CYFRA 21–1 in the six mixed standards were prepared by diluting highly purified CYFRA 21–1 antigen in standard buffer both as 0, 5, 25, 100 and 1000 ng/mL.

Samples and Comparison Method

All samples were kindly provided by Nanfang Hospital (Guangzhou, China) with the CYFRA 21–1 values measured by chemiluminescence immunoassay (CLIA) (Abbott, IL, USA). All the patients were diagnosed on the basis of characteristic clinical features and confirmed by laboratory tests. These samples were stored at −20 °C.

Assay Protocol

The proposed immunoassay for the quantitation of CYFRA 21–1 was performed based on a sandwich type immunoassay format by combining a TRFIA assay and immunomagnetic separation, and was shown schematically in Fig. 1. Initially, 30 μL of standards or samples were added to each well, then 50 μL of magnetic nanoparticles coated with anti-CYFRA 21–1 McAb were added, followed by the addition of 50 μL of assay buffer containing 300 ng Eu^{3+}-labeled anti-CYFRA 21–1 McAb. The mixtures were subsequently incubated at room temperature for 45 min with continuous gentle stirring. Subsequently, the formed sandwich immunocomplexes were drawn to bottom of the test wells and separated from free substances by the application of a samarium–cobalt magnet. After removing the free substances and rinsing with washing buffer four times, 100 μL of enhancement solution was added and then the immunocomplexes were resuspended in enhancement solution and the mixtures were incubated for 5 min at room temperature with stirring. Finally, the fluorescence signal was measured using a Victor^3 1420 Multi-label Counter. The fluorescence of Eu^{3+} was measured at an excitation wavelength of 340 nm and an emission wavelength of 615 nm.

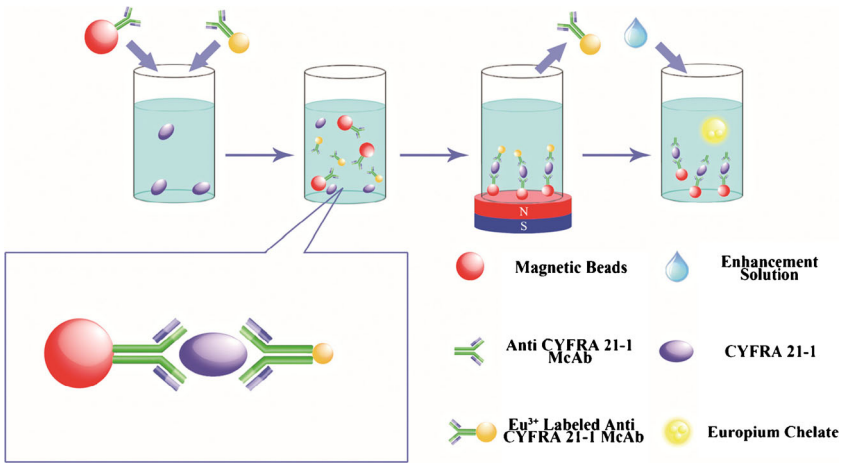

Fig. 1 Example of a magnetic nanoparticle-based TRFIA employing europium chelate label for determination of CYFRA 21–1

Validation Experiment

Preliminary estimates of the lower limit of quantitation (LLOQ) were determined by identifying the lowest concentrations, for which the two-sided 90 % SFSTP (Societe Francaise Sciences et Techniques Pharmaceutiques) confidence limits for percent relative error (RE) were within 25 % of the nominal value as described by Findlay et al. [33]. We spiked standard buffer with purified CYFRA 21–1 to obtain 7 preparations with final concentrations of 0.2–20 ng/mL. Each preparation was aliquoted (n=20) and stored at −70 °C. An aliquot of each preparation was thawed and analyzed each day. This procedure was repeated in 20 independent assays on different days. The bias was defined as the difference between the overall mean of the measurements $(\overline{X})$ and the nominal value (Z). Estimated variance of $\overline{X}(S_{\overline{x}})$ was determined by between-run ANOVA mean square errors. RE (%) including both bias and imprecision was estimated with the equation: $RE = ({}^{100}/_{Z})\cdot[(\overline{X}-Z) \pm t_{0.10/2,\upsilon}\cdot S_{\overline{x}}]$, and the LLOQ was defined as the concentration where RE is 25 % [28, 34]. Dilution linearity of assay was determined using serial dilutions from 2-fold to 16-fold with standard buffer for serum samples. High-dose signal saturation was performed in the range from 5 to 2 000 ng/mL for CYFRA 21–1. The analytical recovery was studied by adding purified CYFRA 21–1 antigen to serum samples. Serum samples were measured using the same batch of reagents on separate days for the evaluation of precision.

Statistical Analyses

Analysis of data was performed using SPSS 13.0 (Chicago, IL, USA). Standard curves were obtained by plotting the fluorescence intensity (Y) against the logarithm of the sample concentration (X) and fitted to a four-parameter logistic equation using Origin7.5 SR1 (Microcal, USA): $LogY = A + B \times LogX$.

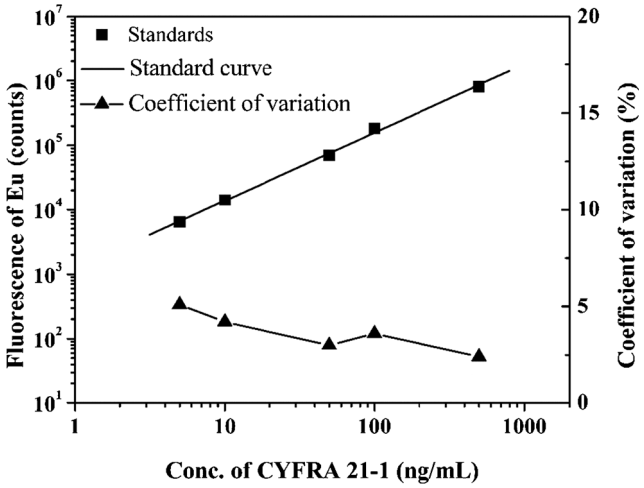

Fig. 2 Standard curve and intra-assay precision profile of our novel assay for CYFRA 21–1. Each point was based on 10 replicates

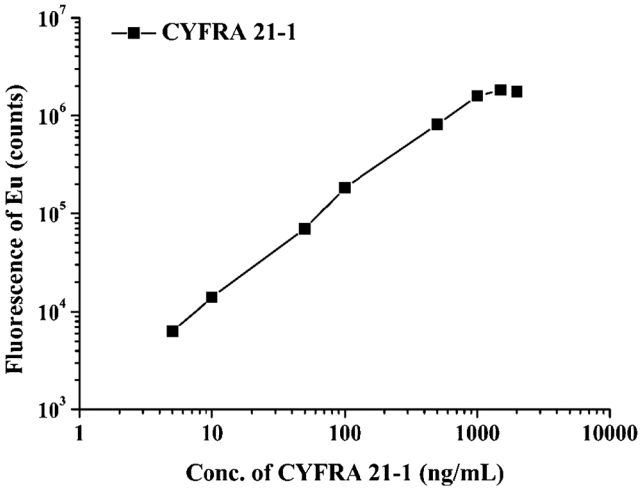

Fig. 3 High-dose signal saturation (hook-effect) of our novel assay for CYFRA 21–1

Results

Standard Curve, Signal Saturation and Lower Limit of Quantitation of the Assay

A standard curve for the immunoassay was carried out following our protocol with a series of dilution of standards (0, 5, 25, 100, 500 and 1000 ng/mL) obtained from 10 separate assays. Standard curve determinations were carried out using linear regression and log-log regression. For the standard curve depicted in Fig. 2, the best-fit calibration was determined to be described by the following equation: $LogY = 3.08 + 1.06 \times LogX$ (r^2=0.996, P<0.0001). Signal saturation ("hook" effect) was seen when the range exceeded 1000 ng/mL (Fig. 3). Within-assay coefficients of variation (n=10) using standards were less than 10 % in the range. Graphical

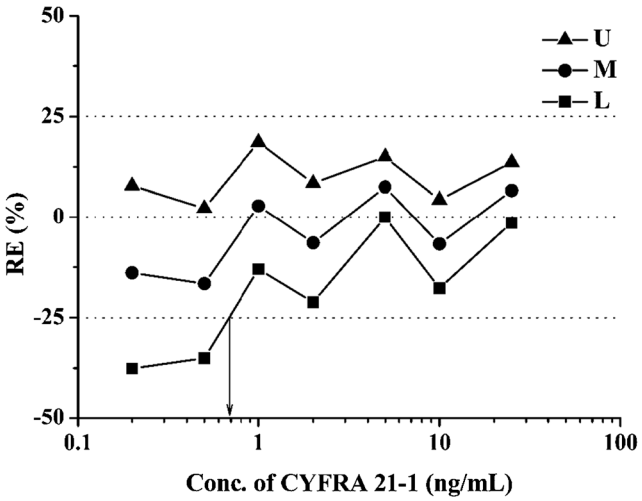

Fig. 4 Total error was plotted as the mean bias (M) ± the 90 % confidence limits of imprecision (U, L), and the LLOQ for CYFRA 21–1 was defined as the concentrations where RE is 25 %

Table 1 Analytical recovery of CYFRA 21–1 added to serum samples

Sample (ng/mL)	CYFRA 21–1 (ng/mL)		
	Expected	Observed	Recovery
21.6	100	101.5	101.5 %
	200	197.6	98.8 %
	400	421.6	105.4 %
30.1	100	98.6	98.6 %
	200	210.2	105.1 %
	400	405.9	101.5 %
62.3	100	98.7	98.7 %
	200	196.3	98.2 %
	400	418.4	104.6 %

CYFRA 21–1 cytokeratin 19 fragment

estimation indicates the lower limit of quantitation of the present method for CYFRA 21–1 was 0.78 ng/ml (Fig. 4).

Analytical Recovery

The analytical recovery was studied by adding purified CYFRA 21–1 antigen to 3 serum samples from different patients. The results are given in Table 1. The recoveries of added analytes were in the range of 90–110 %.

Imprecision

Within-and between-assays imprecision were determined using three serum samples and the same batch of reagents on separate days as showed in Table 2. Total imprecision of the present TRFIA assay were ranged from 3.9 to 6.9 % for CYFRA 21–1.

Dilution

Table 3 gives the results of our evaluation of the dilution linearity of our novel TRFIA when we used samples serially diluted with assay buffer. Expected values were derived from initial concentrations of analytes in the undiluted samples. Correlating the results obtained from our novel TRFIA with the expected concentrations, we found that the dilution curves were linear over the whole range of concentrations. Expected and measured values were well correlated.

Table 2 Precision of our novel assay

	Sample	CYFRA 21–1 (ng/mL)		
		Mean	SD	CV
Within-run (n=12)	1	17.3	0.67	3.9 %
	2	45.9	2.82	6.2 %
	3	82.5	4.05	4.9 %
Between-run (n=15)	1	18.1	1.03	5.6 %
	2	47.3	3.14	6.6 %
	3	84.2	5.83	6.9 %

CV coefficient of variation; *SD* standard deviation; *CYFRA 21–1* cytokeratin 19 fragment

Table 3 Dilution Linearity of our novel assay for CYFRA 21-1

Sample	Dilution	CYFRA 21–1 (ng/mL)		
		Expected	Observed	Recovery
1	NA		39.2	
	1:2	19.6	20.1	102.6 %
	1:4	9.80	9.65	98.5 %
	1:8	4.90	4.98	101.6 %
	1:16	2.45	2.55	104.1 %
2	NA		80.7	
	1:2	40.4	39.5	97.8 %
	1:4	20.2	21.1	104.5 %
	1:8	10.1	9.8	97.0 %
	1:16	5.05	5.12	101.4 %
3	NA		146.8	
	1:2	73.4	73.9	100.7 %
	1:4	36.7	37.3	101.6 %
	1:8	18.4	17.9	97.3 %
	1:16	9.18	9.32	101.5 %

NA not applicable; *CYFRA 21–1* cytokeratin 19 fragment

Comparison with CLIA

CYFRA 21–1 in 90 clinical samples were analyzed by the present TRFIA. The correlation of the CYFRA 21–1 values obtained by this method and those obtained by CLIA was

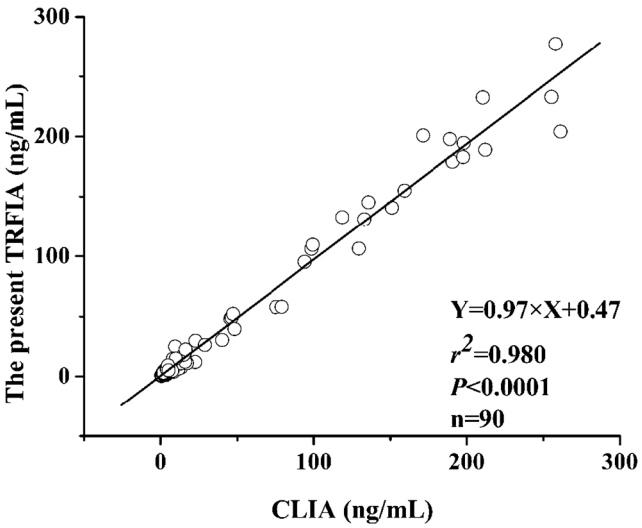

Fig. 5 Graphical comparisons of the present TRFIA and CLIA results for determination of CYFRA 21–1

excellent; the regression equation was $Y = 0.97 \times X + 0.47$ (r^2=0.980, P<0.0001). The comparison of CYFRA 21–1 values obtained by the two methods (TRFIA and CLIA) was shown in Fig. 5.

Discussion

Although the TRFIA holds great promise, limitations in the conventional TRFIA methodology remain. For instance, the specific antigen or antibody is usually immobilized on the plastic surface of 96-well microplates by physical absorption; it is unstable and can be readily washed away. Magnetic nanoparticles as nanometer materials have been successfully employed in many areas of research, including cell separation, biomolecule detection, DNA extraction and various immunoassay methodologies [35–38]. Magnetic nanoparticles with bioactive molecules such as antibodies are very useful tools for immunoassays. Utilizing magnetic nanoparticles-beads could be a key to protect the specific antigen or antibody from being washed away. Unlike conventional TRFIA, antibodies were coupled to the surface of magnetic beads rather than immobilized on the surface of 96-well microplates. The magnetic nanoparticles-beads suspended in the reaction solution provide a relatively larger surface area. This enabled more antibodies to be coupled to the surface, thereby reducing the consumption of reagents and improving the immobilization of more antibodies. This led to appreciable broadening of the linear range of detection. Additionally, antibody-coated magnetic nanoparticles-beads employed as a solid phase in suspension to capture analytes enabled more antigens to become accessible within a short time. Hence, antigen–antibody equilibrium could be achieved more rapidly, which further reduced the analysis time.

With the rapid development of clinical diagnosis, the combined applications of serum tumor markers are paid more and more attention by the researchers. Based on the application of magnetic nanoparticles and dual-label, magnetic nanoparticle-based dual-label TRFIA had been noticed as a highly sensitive method and employed in numerous applications for simultaneous determination of multiple analytes [31, 32]. The extension of the present TRFIA to the simultaneous detection of additional multiple analytes is currently under investigation. For instance, we have focused on a magnetic particle-based dual-label time-resolved fluoroimmunoassay for simultaneous determination of the carcinoembryonic antigen and CYFRA 21–1 in human serum.

Conclusions

In summary, we have developed a novel magnetic nanoparticle-based TRFIA, which was designed specifically as a sensitive, precise and rapid measurement method for determination of the CYFRA 21–1 in human serum. The present method established here, when applied to the determination of CYFRA 21–1 in human serum, showed excellent correlation with the conventional CLIA kit. Additionally, this novel method demonstrated high sensitivity, wider effective detection range and excellent reproducibility for the determination of CYFRA 21–1, and offered the additional benefit of faster detection, resulting in a substantially faster assay. Our novel assay can be useful for early screening and prognosis evaluation of patients with NSCLC by minimizing time and investment cost. Based on this investigation, we established a good foundation for further development of other biomarkers using the same platform.

Acknowledgments The work was supported by the National Natural Science Foundation of China (Grant No. 81271931) and the Natural Science Foundation of Guangdong Province (Grant No. S2012010009547).

References

1. Jemal A, Siegel R, Ward E, Hao Y, Xu J, Thun MJ (2009) Cancer statistics, 2009. CA Cancer J Clin 59(4):225–249
2. Strauss GM, Herndon JE 2nd, Maddaus MA, Johnstone DW, Johnson EA, Harpole DH, Gillenwater HH, Watson DM, Sugarbaker DJ, Schilsky RL, Vokes EE, Green MR (2008) Adjuvant paclitaxel plus carboplatin compared with observation in stage IB non-small-cell lung cancer: CALGB 9633 with the Cancer and Leukemia Group B, Radiation Therapy Oncology Group, and North Central Cancer Treatment Group Study Groups. J Clin Oncol 26(31):5043–5051
3. Goya T, Asamura H, Yoshimura H, Kato H, Shimokata K, Tsuchiya R, Sohara Y, Miya T, Miyaoka E, Japanese Joint Committee of Lung Cancer R (2005) Prognosis of 6644 resected non-small cell lung cancers in Japan: a Japanese lung cancer registry study. Lung Cancer 50(2):227–234
4. Hanagiri T, Baba T, So T, Yasuda M, Sugaya M, Ono K, So T, Uramoto H, Takenoyama M, Yasumoto K (2010) Time trends of surgical outcome in patients with non-small cell lung cancer. J Thorac Oncol 5(6):825–829
5. Schiller JH (2001) Current standards of care in small-cell and non-small-cell lung cancer. Oncology 61(Suppl 1):3–13
6. Hanagiri T, Sugaya M, Takenaka M, Oka S, Baba T, Shigematsu Y, Nagata Y, Shimokawa H, Uramoto H, Takenoyama M, Yasumoto K, Tanaka F (2011) Preoperative CYFRA 21–1 and CEA as prognostic factors in patients with stage I non-small cell lung cancer. Lung Cancer 74(1):112–117
7. Mulshine JL, Sullivan DC (2005) Clinical practice. Lung cancer screening. N Engl J Med 352(26):2714–2720
8. Wang P, Piao Y, Zhang X, Li W, Hao X (2013) The concentration of CYFRA 21–1, NSE and CEA in cerebro-spinal fluid can be useful indicators for diagnosis of meningeal carcinomatosis of lung cancer. Cancer Biomark 13(2):123–130
9. Pujol JL, Grenier J, Daures JP, Daver A, Pujol H, Michel FB (1993) Serum fragment of cytokeratin subunit 19 measured by CYFRA 21–1 immunoradiometric assay as a marker of lung cancer. Cancer Res 53(1):61–66

10. Vollmer RT, Govindan R, Graziano SL, Gamble G, Garst J, Kelley MJ, Christenson RH (2003) Serum CYFRA 21–1 in advanced stage non-small cell lung cancer: an early measure of response. Clin Cancer Res 9(5):1728–1733
11. Ando S, Kimura H, Iwai N, Yamamoto N, Iida T (2003) Positive reactions for both Cyfra21-1 and CA125 indicate worst prognosis in non-small cell lung cancer. Anticancer Res 23(3C):2869–2874
12. Reinmuth N, Brandt B, Semik M, Kunze WP, Achatzy R, Scheld HH, Broermann P, Berdel WE, Macha HN, Thomas M (2002) Prognostic impact of Cyfra21-1 and other serum markers in completely resected non-small cell lung cancer. Lung Cancer 36(3):265–270
13. Ando S, Suzuki M, Yamamoto N, Iida T, Kimura H (2004) The prognostic value of both neuron-specific enolase (NSE) and Cyfra21-1 in small cell lung cancer. Anticancer Res 24(3b):1941–1946
14. Pujol JL, Quantin X, Jacot W, Boher JM, Grenier J, Lamy PJ (2003) Neuroendocrine and cytokeratin serum markers as prognostic determinants of small cell lung cancer. Lung Cancer 39(2):131–138
15. Holdenrieder S, Von Pawel J, Duell T, Feldmann K, Raith H, Schollen A, Nagel D, Stieber P (2010) Clinical relevance of thymidine kinase for the diagnosis, therapy monitoring and prognosis of non-operable lung cancer. Anticancer Res 30(5):1855–1862
16. Takada M, Masuda N, Matsuura E, Kusunoki Y, Matui K, Nakagawa K, Yana T, Tuyuguchi I, Oohata I, Fukuoka M (1995) Measurement of cytokeratin 19 fragments as a marker of lung cancer by CYFRA 21–1 enzyme immunoassay. Br J Cancer 71(1):160–165
17. Chapman MH, Sandanayake NS, Andreola F, Dhar DK, Webster GJ, Dooley JS, Pereira SP (2011) Circulating CYFRA 21–1 is a specific diagnostic and prognostic biomarker in biliary tract cancer. J Clin Exp Hepatol 1(1):6–12
18. Kuropkat C, Werner JA (2003) Analytical and clinical evaluation of CYFRA 21–1 by electrochemiluminescent immunoassay in head and neck squamous cell carcinoma. J Laryngol Otol 117(12):1007–1008, author reply 1008–1009
19. Zhu L, Xu L, Jia N, Huang B, Tan L, Yang S, Yao S (2013) Electrochemical immunoassay for carcinoembryonic antigen using gold nanoparticle–graphene composite modified glassy carbon electrode. Talanta 116:809–815
20. Lovgren T, Hemmila I, Pettersson K, Eskola JU, Bertoft E (1984) Determination of hormones by time-resolved fluoroimmunoassay. Talanta 31(10 Pt 2):909–916
21. Hemmila I, Dakubu S, Mukkala VM, Siitari H, Lovgren T (1984) Europium as a label in time-resolved immunofluorometric assays. Anal Biochem 137(2):335–343
22. Dickson EF, Pollak A, Diamandis EP (1995) Ultrasensitive bioanalytical assays using time-resolved fluorescence detection. Pharmacol Ther 66(2):207–235
23. Hemmila I (1985) Fluoroimmunoassays and immunofluorometric assays. Clin Chem 31(3):359–370
24. Kricka LJ (1994) Selected strategies for improving sensitivity and reliability of immunoassays. Clin Chem 40(3):347–357
25. Adlercreutz H, Wang GJ, Lapcik O, Hampl R, Wahala K, Makela T, Lusa K, Talme M, Mikola H (1998) Time-resolved fluoroimmunoassay for plasma enterolactone. Anal Biochem 265(2):208–215
26. Huo T, Wang L, Liu L, Chu X, Xu C (2006) Rapid time-resolved fluoroimmunoassay for diethylstilbestrol residues in chicken liver. Anal Biochem 357(2):272–276
27. Lin GF, Liu TC, Zou LP, Hou JY, Wu YS (2013) Development of a dual-label time-resolved fluoroimmunoassay for the detection of alpha-fetoprotein and hepatitis B virus surface antigen. Luminescence 28(3):401–406
28. Lin G, Huang H, Liu T, He C, Liu J, Chen S, Hou J, Ren Z, Dong W, Wu Y (2014) A time-resolved fluoroimmunoassay for the quantitation of rabies virus nucleoprotein in the rabies vaccine. J Virol Methods 206:89–94
29. Hou JY, Liu TC, Lin GF, Li ZX, Zou LP, Li M, Wu YS (2012) Development of an immunomagnetic bead-based time-resolved fluorescence immunoassay for rapid determination of levels of carcinoembryonic antigen in human serum. Anal Chim Acta 734:93–98
30. Ren ZQ, Liu TC, Hou JY, Chen MJ, Chen ZH, Lin GF, Wu YS (2013) A rapid and sensitive method based on magnetic beads for the detection of hepatitis B virus surface antigen in human serum. Luminescence 29(6):591–7
31. Hou JY, Liu TC, Ren ZQ, Chen MJ, Lin GF, Wu YS (2013) Magnetic particle-based time-resolved fluoroimmunoassay for the simultaneous determination of alpha-fetoprotein and the free beta-subunit of human chorionic gonadotropin. Analyst 138(13):3697–3704
32. Liu TC, Chen MJ, Ren ZQ, Hou JY, Lin GF, Wu YS (2014) Development of an improved time-resolved fluoroimmunoassay for simultaneous quantification of C-peptide and insulin in human serum. Clin Biochem 47(6):439–444
33. Findlay JW, Smith WC, Lee JW, Nordblom GD, Das I, DeSilva BS, Khan MN, Bowsher RR (2000) Validation of immunoassays for bioanalysis: a pharmaceutical industry perspective. J Pharm Biomed Anal 21(6):1249–1273
34. De Pauw PE, Vermeulen I, Ubani OC, Truyen I, Vekens EM, van Genderen FT, De Grijse JW, Pipeleers DG, Van Schravendijk C, Gorus FK (2008) Simultaneous measurement of plasma concentrations of proinsulin and C-peptide and their ratio with a trefoil-type time-resolved fluorescence immunoassay. Clin Chem 54(12):1990–1998
35. Tokairin T, Nishikawa Y, Doi Y, Watanabe H, Yoshioka T, Su M, Omori Y, Enomoto K (2002) A highly specific isolation of rat sinusoidal endothelial cells by the immunomagnetic bead method using SE-1 monoclonal antibody. J Hepatol 36(6):725–733
36. Careri M, Elviri L, Lagos JB, Mangia A, Speroni F, Terenghi M (2008) Selective and rapid immunomagnetic bead-based sample treatment for the liquid chromatography-electrospray ion-trap mass spectrometry detection of Ara h3/4 peanut protein in foods. J Chromatogr A 1206(2):89–94
37. Wang X, Zhang QY, Li ZJ, Ying XT, Lin JM (2008) Development of high-performance magnetic chemiluminescence enzyme immunoassay for alpha-fetoprotein (AFP) in human serum. Clin Chim Acta 393(2):90–94
38. Lin JY, Chen YC (2011) Functional magnetic nanoparticle-based trapping and sensing approaches for label-free fluorescence detection of DNA. Talanta 86:200–207